A Minimum-Time Optimal Recharging Controller for High Pressure Gas Storage Systems

Kenneth R. Muske, Amanda E. Witmer, and Randy D. Weinstein

Department of Chemical Engineering, Villanova University, Villanova, PA, 19085, USA
kenneth.muske@villanova.edu

Summary. A minimum-time optimal recharging control strategy for high pressure gas storage tank systems is described in this work. The goal of the nonlinear model-based controller is to refill the tank in minimum time with a two-component gas mixture of specified composition subject to hard constraints on the component flow rates, tank temperature, and tank pressure. The nonlinearity in this system arises from the non-ideal behavior of the gas at high pressure. The singular minimum-time optimal control law can not be reliably implemented in the target application due to a lack of sensors. Minimum-time optimal control is therefore approximated by a nonlinear model-based constraint controller. In order to account for the uncertainty in the unmeasured state of the storage tank, the state sensitivities to the control and process measurements are propagated along with the state to obtain a state variance estimate. When the variance of the state exceeds a maximum threshold, the constraint control algorithm automatically degrades into a fail-safe operation.

1 Introduction

The gas storage tank recharging system, shown in Figure 1, consists of high pressure sources for each component that supply the gas to the storage tanks. A source pressure sensor and mass flow controller are available for each component. A pressure sensor upstream of the discharge nozzle into the storage tank and an ambient temperature sensor are the only other process measurements. There are no sensors in the storage tank itself because of economic and maintenance reasons. It is less expensive to instrument the supply line from the tank than to replicate and maintain these instruments in each tank.

The controlled variables for this system are the final mass, or total moles, and composition of the gas in the storage tank. The manipulated variables are the setpoints to the component mass flow controllers. The system may be operated by either maintaining the feed gas at the desired composition during the entire refilling process or allowing the feed gas composition to vary with the desired composition being achieved when the tank is refilled. In this work, the first operating philosophy will be adopted. The advantage of the first approach is that the gas in the tank is always at the desired composition. If the refilling process must be terminated for any reason, the storage tank will still have the

R. Findeisen et al. (Eds.): Assessment and Future Directions, LNCIS 358, pp. 443–453, 2007.
springerlink.com

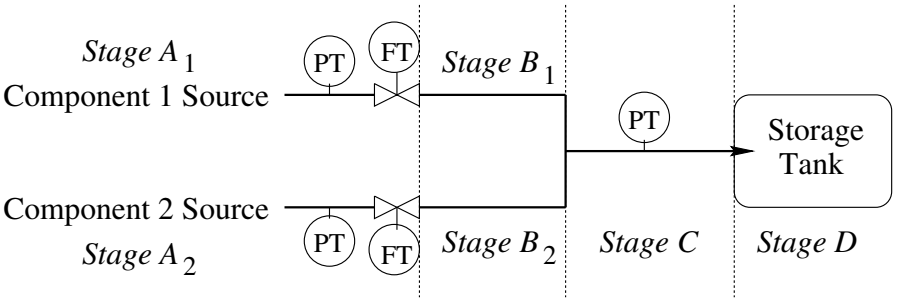

Fig. 1. Gas storage tank recharging system

correct composition. The disadvantage of this approach is that the controller can not use the extra degree of freedom to take advantage of any differences in the component gas properties when refilling the tank.

The objective of the control system is to safely fill the gas storage tank in minimum time with a specified amount of a two-component gas mixture subject to pressure and temperature constraints. Of particular concern in this process is the Joule–Thompson behavior of the gas components comprising the mixture. For systems with a positive Joule–Thompson coefficient, the gas mixture will cool as it expands from source pressure into the storage tank. In this case, the maximum pressure constraint must be lowered to account for the future increase in pressure as the system reaches ambient temperature. For systems with a negative Joule-Thompson coefficient, the gas mixture temperature will rise as the storage tank is filled. In this case, the rate of temperature rise must be controlled to reach the desired final amount without exceeding the maximum temperature limit of the storage tank and delivery system. Over the pressure ranges of interest, however, some gas components can exhibit significant changes in the Joule–Thompson coefficient including sign changes.

2 Thermodynamic Model

The recharging system model is based on the thermodynamic relationships for the transition between each of the four stages shown in Figure 1. The first two stage transitions, A $\rightarrow$ B and B $\rightarrow$ C, are modeled as isoenthalpic transitions with no gas accumulation. The result is a series of steady-state algebraic equations relating the temperature, pressure, and density at each stage. The last stage transition, C $\rightarrow$ D, is modeled using an isoentropic transition through the nozzle and an unsteady-state energy balance over the storage tank. The result is a differential-algebraic system where the algebraic equations arise from the isoentropic transition and the equation of state.

2.1 Equation of State

The following two-coefficient virial equation of state for a binary mixture [1]

$$Z = \frac{P}{RT\rho} = 1 + B_{\text{mix}}\rho + C_{\text{mix}}\rho^2 \tag{1}$$

$$B_{\text{mix}} = b_1(T)x_1^2 + 2b_{12}(T)x_1x_2 + b_2(T)x_2^2 \tag{2}$$

$$C_{\text{mix}} = c_1(T)x_1^3 + 3c_{112}(T)x_1^2x_2 + 3c_{122}(T)x_1x_2^2 + c_2(T)x_2^3 \tag{3}$$

is used in this work where x_1, x_2 are the component mole fractions and B_{mix} and C_{mix} are, in general, functions of temperature. Because the composition of the inlet gas mixture is maintained at the desired target composition, x_1 and x_2 are constant at this composition in stages C and D. The equation of state for the single component streams in stages A_1 and B_1 is obtained by setting $x_1 = 1$ and $x_2 = 0$ in Eqs. 2 and 3. The equation of state for stages A_2 and B_2 is handled in a similar manner by setting $x_1 = 0$ and $x_2 = 1$.

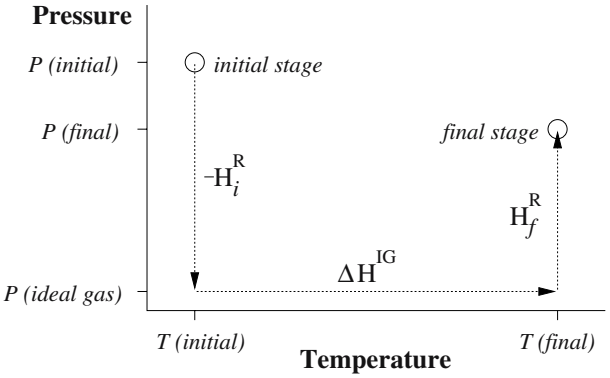

Fig. 2. Isoenthalpic stage transition model

2.2 Isoenthalpic Transition

The first two transitions are described by the path shown in Figure 2 for both the individual pure components and the gas mixture. The resulting equation for the transition from an initial stage i to the next stage f becomes

$$\Delta H_{i\to f} = 0 = -H_i^{\text{R}} + \Delta H^{\text{IG}} + H_f^{\text{R}} \tag{4}$$

where H_i^{R} is the residual enthalpy between the gas at the initial stage and the gas at ideal conditions at the initial temperature, ΔH^{IG} is the change in enthalpy of the gas at ideal conditions between the final and initial temperatures, and H_f^{R} is the residual enthalpy between the gas at the next stage and the gas at ideal conditions at the final temperature. The residual enthalpy is

$$H^{\mathrm{R}} = H - H^{\mathrm{IG}} = -RT^2 \int_0^{\rho_g} \frac{\partial Z(\rho)}{\partial T} \frac{d\rho}{\rho} + RT(Z-1) \tag{5}$$

where H^{IG} is the enthalpy of the gas at ideal conditions (the limit as pressure, or density, goes to zero at the actual temperature), Z is the compressibility, and ρ_g is the gas density [1]. The temperature change and component mixing are done at ideal conditions because the enthalpy of mixing is zero and ideal gas heat capacities, which are only a function of temperature, can be used.

$$\Delta H^{\mathrm{IG}} = \Delta H^{\mathrm{IG}}_{\mathrm{mix}} + \int_{T_i}^{T_f} C_p \, dT \; = \int_{T_i}^{T_f} C_p \, dT \tag{6}$$

The ideal gas heat capacity is taken as an empirical function of temperature.

$$C_p = \sum_{j=1}^{2} x_j C_{p_j} = R \sum_{j=1}^{2} x_j \left(\alpha_j + \beta_j T + \gamma_j T^2 + \epsilon_j T^{-2} \right) \tag{7}$$

2.3 Isoentropic Transition

If we assume a perfect nozzle, and therefore isoentropic flow, the transition from stage C to stage D can be described by the transition $\Delta S_{C \to D} = 0$ or by the relationship for isentropic adiabatic flow through a nozzle. The complexity arising from a nonideal gas with sonic flow for some fraction of the time suggests abandoning the flow equation in favor of the entropy relationship

$$\Delta S_{C \to D} = 0 = -S^{\mathrm{R}}_C + \Delta S^{\mathrm{IG}} + S^{\mathrm{R}}_D \tag{8}$$

$$S^{\mathrm{R}} = S - S^{\mathrm{IG}} = R \left[\ln Z - T \int_0^{\rho_g} \left(\frac{\partial Z(\rho)}{\partial T} - \frac{Z(\rho) - 1}{T} \right) \frac{d\rho}{\rho} \right] \tag{9}$$

$$\Delta S^{\mathrm{IG}} = \int_{T_C}^{T_D} C_p \frac{dT}{T} - \int_{P_C}^{P_D} R \frac{dP}{P} \tag{10}$$

where S^{R} is the residual entropy and ΔS^{IG} is the change in enthalpy at ideal conditions [1]. The result is analogous to the enthalpy relationships in Eqs. 4–6 except there is no mixing term because the stage compositions are the same.

2.4 Unsteady-State Energy Balance

The unsteady-state energy balance for the gas mixture in the storage tank is

$$n_D \left[\frac{dH_D}{dt} + \frac{d}{dt} \left(\frac{P_D}{\rho_D} \right) \right] - \dot{n}_D \left[\Delta H_{C \to D} + \frac{P_D}{\rho_D} \right] - \dot{Q}_D = 0 \tag{11}$$

where n_D is the total moles of gas in the storage tank, $\rho_D = n_D / V_D$ is the density of the gas in the tank, V_D is the tank volume, H_D is the enthalpy of

the gas mixture in the storage tank, $\Delta H_{C\to D}$ is the change in enthalpy between the gas mixture upstream of the nozzle and the gas in the storage tank, $\dot{Q}_D$ is the heat transfered from the storage tank to the surroundings, and the rate of change of the moles of gas in the tank is determined by the control $\dot{n}_D = u$. Because the composition of the inlet gas mixture is maintained at the desired target composition, the total molar flow rate is the single control.

The rate of change of the enthalpy of the gas inside the storage tank is

$$\frac{dH_D}{dt} = \frac{\partial H_D}{\partial T}\frac{dT_D}{dt} + \frac{\partial H_D}{\partial \rho}\frac{d\rho_D}{dt} = \left(C_{p_D} + \frac{\partial H_D^{\mathrm{R}}}{\partial T}\right)\frac{dT_D}{dt} + \left(\frac{\rho_D}{n_D}\frac{\partial H_D^{\mathrm{R}}}{\partial \rho}\right)u \quad (12)$$

where the residual enthalpy H_D^{R} is as defined in Eq. 5. The rate of change of P_D/ρ_D can be expressed as a function of the temperature change as follows.

$$\frac{d}{dt}\left(\frac{P_D}{\rho_D}\right) = \frac{d}{dt}(RZ_DT_D) = R\left(Z_D + T_D\frac{\partial Z_D}{\partial T}\right)\frac{dT_D}{dt} + R\left(\frac{T_D\rho_D}{n_D}\frac{\partial Z_D}{\partial \rho}\right)u \quad (13)$$

2.5 Differential-Algebraic System Model

The preceding thermodynamic relationships result in the following differential algebraic modeling equations for the system where we will assume that $\dot{Q} = 0$.

$$H_{B_1}^{\mathrm{R}} + \int_{T_{A_1}}^{T_{B_1}} C_{p_1}\,dT - H_{A_1}^{\mathrm{R}} = 0 \quad (14)$$

$$P_{B_1} - RT_{B_1}\left(\rho_{B_1} + B_{\mathrm{mix}}\rho_{B_1}^2 + C_{\mathrm{mix}}\rho_{B_1}^3\right) = 0 \quad (15)$$

$$H_{B_2}^{\mathrm{R}} + \int_{T_{A_2}}^{T_{B_2}} C_{p_2}\,dT - H_{A_2}^{\mathrm{R}} = 0 \quad (16)$$

$$P_{B_2} - RT_{B_2}\left(\rho_{B_2} + B_{\mathrm{mix}}\rho_{B_2}^2 + C_{\mathrm{mix}}\rho_{B_2}^3\right) = 0 \quad (17)$$

$$H_C^{\mathrm{R}} + x_1\left(\int_{T_{B_1}}^{T_C} C_{p_1}\,dT - H_{B_1}^{\mathrm{R}}\right) + x_2\left(\int_{T_{B_2}}^{T_C} C_{p_2}\,dT - H_{B_2}^{\mathrm{R}}\right) = 0 \quad (18)$$

$$P_C - RT_C\left(\rho_C + B_{\mathrm{mix}}\rho_C^2 + C_{\mathrm{mix}}\rho_C^3\right) = 0 \quad (19)$$

$$S_D^{\mathrm{R}} + \int_{T_C}^{T_D} C_{p_D}\frac{dT}{T} - \int_{P_C}^{P_D} R\frac{dP}{P} - S_C^{\mathrm{R}} = 0 \quad (20)$$

$$n_D - \rho_D V_D = 0 \quad (21)$$

$$P_D - RT_D\left(\rho_D + B_{\mathrm{mix}}\rho_D^2 + C_{\mathrm{mix}}\rho_D^3\right) = 0 \quad (22)$$

$$\frac{H_D^{\mathrm{R}} + \int_{T_C}^{T_D} C_{p_D} dT - H_C^{\mathrm{R}} + \frac{P_D}{\rho_D} - \left(\frac{\partial H_D^{\mathrm{R}}}{\partial \rho} + RT_D \frac{\partial Z_D}{\partial \rho}\right)\rho_D}{n_D\left(C_{p_D} + \frac{\partial H_D^{\mathrm{R}}}{\partial T} + R\left(Z_D + T_D \frac{\partial Z_D}{\partial T}\right)\right)} u = \dot{T}_D \qquad (23)$$

$$u = \dot{n}_D \qquad (24)$$

There are two differential and nine algebraic equations in Eqs. 14–24 for the thirteen unknowns: P, T, & ρ for stages B_1, B_2, C, & D and n_D. Making the assumption that $P_{B_1} = P_{B_2} = P_C$ reduces the number of unknowns to eleven.

3 Minimum-Time Optimal Control

The optimization problem for the minimum-time optimal controller is

$$\min_{u(t)} \int_{t=0}^{t_f} 1\, dt \quad \text{Subject to:} \quad \begin{aligned} & n_D(t_f) = n_D^\star \\ & \dot{x} = f(x)u \\ & g(x) = 0 \\ & h_x(x) \le 0 \\ & h_u(u) \le 0 \end{aligned} \qquad (25)$$

where x is the system state, u is the control, $n_D^\star$ is the desired final moles of gas in the storage tank, $f(x)u$ represents the differential equations in Eqs. 23–24, $g(x)$ represents the algebraic equations in Eqs. 14–22, $h_x(x)$ represents the tank temperature and pressure hard constraints, and $h_u(u)$ represents the component gas flow rate hard constraints. As is common for minimum-time problems, the result is a singular optimal control problem. The optimal control trajectory is either at a constraint, from the minimum principle, or along an optimal singular arc that satisfies the Euler–Lagrange equations [2].

Because the enthalpy of the gas in the tank is a state function, the isoentropic assumption for the stage C to stage D transition neglects losses in the inlet line, and the system is assumed adiabatic, the state of the storage tank determined from the differential-algebraic system model presented in Eqs. 14–24 is path independent. Therefore, all control profiles result in the same final tank state for a given final moles of gas $n_D^\star$. If a steady-state analysis determines that a tank constraint is violated at this target, then there is no feasible control profile $u(t)$ that satisfies both the terminal equality constraint $n_D(t_f) = n_D^\star$ and the tank state inequality constraints $h_x(x) \le 0$ for the minimum-time optimal control problem in Eq. 25. In this case, an alternative feasible optimal control approach would be to construct a singular optimal controller that achieves the most limiting tank constraint in minimum time.

An excellent review of solution methods for singular optimal control problems arising from batch processes is presented in [3]. The use of process measurements to improve the robustness of optimal control to model mismatch and unmeasured disturbances is discussed in [4]. The application of these techniques to the controller in this work, however, is restricted by the lack of process measurements.

With only a single pressure measurement to estimate eleven states, state feedback is either impossible (if the integrating state is not detectable) or highly unreliable (because of the variance in the state estimates). Open-loop optimal control approaches, discussed in [5], are inappropriate in this application due to the consequences of a constraint violation. For these reasons, a model-based dynamic constraint controller is proposed.

4 Model-Based Dynamic Constraint Control

We develop a model predictive dynamic constraint controller to approximate the minimum-time optimal recharging controller presented in the previous section. The single process measurement, inlet line pressure, is integrated into the constraint controller by using this measurement to eliminate the isoentropic relationship $\Delta S_{C\to D} = 0$ (Eq. 20) from the model. The advantage of this integration is that the isoentropic transition assumption is removed from the model which also removes the path independence of the tank state. The disadvantage of this approach is that there is no output feedback correction to the tank state. However, it is unlikely that state estimation based on the single pressure measurement would result in any significant improvement in the model predicted tank state. The uncertainty in the tank state prediction can be monitored by estimating the variance as outlined in the sequel.

The model-based dynamic constraint controller attempts to drive the system to the most limiting constraint in minimum time while relaxing the terminal state equality constraint $n_D(t_f) = n_D^\star$ if necessary. The dynamic constraint controller is a model predictive version of the active constraint tracking controller in [6]. This control structure is motivated by the solution to the feasible minimum-time optimal control problem in the previous section which specifies that the system should be operated at an active constraint during the entire refilling process. We note that if the irreversible losses in the system are negligible, then open-loop optimal control, closed-loop model predictive control, and closed-loop dynamic constraint control should all result in this same active constraint tracking input trajectory. If irreversible losses are significant, then constraint control may not be a good approximation to the optimal input trajectory. Preliminary experimental evidence suggests the former case [7].

4.1 Constraint Controller

Constraint prediction is performed by solving the DAE system in Eqs. 14–19, 21–24 from the initial time to the current time using the past control and inlet pressure measurement trajectories. The initial state of the system is available from the ambient temperature measurement and the initial inlet line pressure which is the same as the tank pressure at zero flow. The future state predictions are then obtained by assuming that the control and inlet line pressure remain

constant at their current values until the tank is refilled. The target final moles of gas in the tank is determined at each sample period k by

$$n_D^{\mathrm{F}}(k) = \min\left[n_D^{\star},\, n|_{T_D=T_D^{\max}}(k),\, n|_{T_D=T_D^{\min}}(k),\, n|_{P_D=P_D^{\max}}(k)\right] \tag{26}$$

where $n_D^{\mathrm{F}}(k)$ is the current target final moles of gas at sample period k, $n_D^{\star}$ is the desired final moles of gas, $n|_{T_D=T_D^{\max}}$ is the current predicted moles of gas such that the tank temperature reaches its maximum constraint limit, $n|_{T_D=T_D^{\min}}$ is the current predicted moles of gas such that the tank temperature reaches its minimum constraint limit, $n|_{P_D=P_D^{\max}}$ is the current predicted moles of gas such that the tank pressure reaches its maximum constraint limit, and the *min* operator selects the most limiting model-predicted constraint. The current predicted moles of gas required to reach a tank constraint is determined directly from the predicted future tank state profile. The length of the prediction horizon is always the time required to obtain $n_D^{\star}$ moles of gas in the tank. If a constraint violation is not predicted within this horizon, it is not considered by the *min* operator in Eq. 26. A first-order approximation to the control move required to achieve the most limiting constraint in minimum time is then determined from the current predicted tank state and target by

$$u(k) = \min\left[u^{\max}, \frac{n_D^{\mathrm{F}}(k) - n_D(k)}{\Delta t}\right] \tag{27}$$

where $u(k)$ is the current input, $u^{\max}$ is the maximum flow rate constraint, and $n_D(k)$ is the current prediction of the moles of gas in the storage tank.

This dynamic constraint prediction is computed at every sample period after the initial start-up phase. The start up is carried out at a minimum safe gas flow rate to ensure that the system is operating properly. The constraint prediction is updated by the incorporation of the most recent inlet pressure measurement at the current sample time. We note that on-line optimization is not required to determine the control input because of the assumption that the optimal operation is at an active constraint (motivated by the minimum-time optimal control trajectory). Because the DAE system and the state sensitivities, required for the uncertainty estimate described in the next section, can be computed very quickly, the sample period Δt is not limited by computational issues as is often the case for nonlinear predictive control implementations.

4.2 Fail-Safe Operation

Because there is no direct measurement of the actual tank state, some mechanism to monitor the uncertainty in this state estimate is required for the safe implementation of the proposed controller. Linear approximations to the variance of the tank state can be obtained from the first-order sensitivities [8] between the tank state and the control and inlet line pressure as follows

$$\sigma_{x,P_C}^2 = \left(\frac{\partial x}{\partial P_C}\right)^2 \sigma_{P_C}^2, \quad \sigma_{x,u}^2 = \left(\frac{\partial x}{\partial u}\right)^2 \sigma_u^2, \quad F = \frac{\sigma_{x,P_C}^2}{\lambda + \sigma_{x,u}^2} > F_\alpha \tag{28}$$

where x is the tank temperature or pressure, the partials are the sensitivities, σ^2_{x,P_C} is the estimate using the pressure measurement variance $\sigma^2_{P_C}$, $\sigma^2_{x,u}$ is the estimate using the control variance σ^2_u, F_α is the F statistic at a confidence level α, λ is a tuning parameter to account for measurement noise and normal variation in the inlet line pressure, and $F > F_\alpha$ implies $\sigma^2_{x,P_C} > \sigma^2_{x,u}$ [9]. If the variance estimated from the inlet line pressure measurement exceeds that estimated from the control, the constraint control is terminated to a fail-safe operation. This operation can either shut off the gas flow completely, where the tank pressure could then be determined by the inlet line pressure sensor, or can reduce the gas flow to a predetermined minimum safe value.

5 Example

The control strategy is illustrated using a nitrogen–helium gas mixture. We choose this system because the sign of the Joule-Thompson coefficient is different for each component; negative for helium and positive for nitrogen. There are also significant differences in the intermolecular potentials leading to large deviations from ideal behavior. The coefficients in Eqs. 2–3 are affine functions of temperature taken from [10]. We consider a 1/4 He/N_2 gas blend in a 100 lit storage tank where the component source pressures are both 175 bar, the ambient temperature is 300 K, and the initial tank pressure is 10 bar. Figure 3 presents the predicted tank temperature profiles for a series of flow rates which clearly demonstrate the nonideal behavior and path independence of the tank state. The predicted pressure profiles behave in a similar manner.

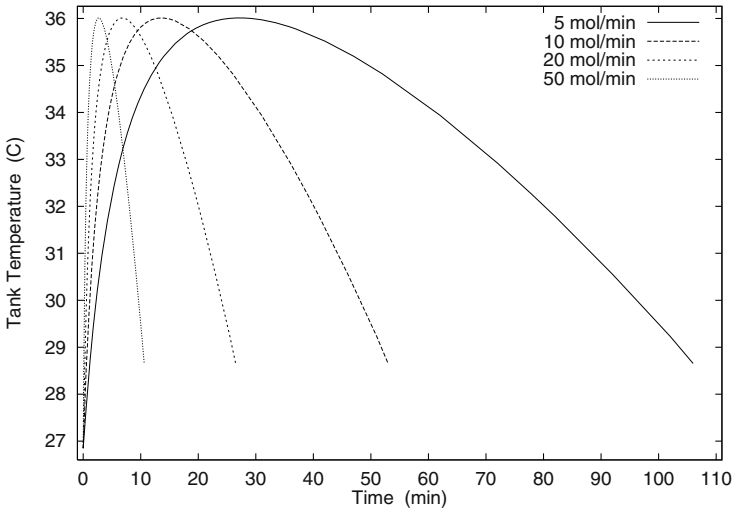

Fig. 3. Predicted tank temperature profiles

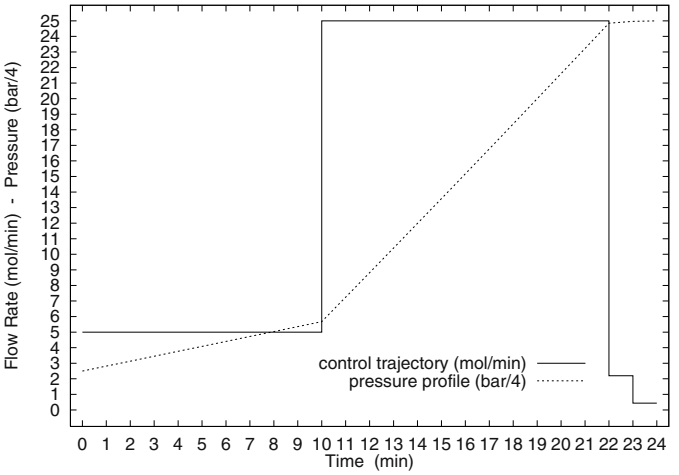

Fig. 4. Control trajectory and simulated tank pressure profile

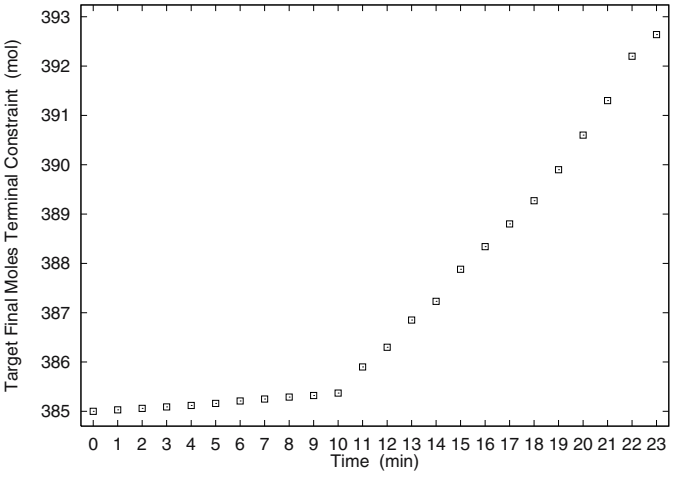

Fig. 5. Target final moles of gas in the tank

We consider a desired value of $n_D^\star = 400$ mol and a maximum operating constraint of $P_D^{\max} = 100$ bar for the tank pressure. At this pressure constraint, only 385 moles of gas can be stored in the tank assuming no thermodynamic losses. Therefore, the maximum tank pressure is the most limiting constraint in this example. The inlet line pressure is simulated using an ideal gas nozzle flow equation with energy loss. The maximum gas flow rate is 25 mol/min. The sample period is one minute. Figure 4 presents the dynamic constraint control trajectory $u(k)$ determined from Eq. 27 and the actual tank pressure. The first

ten minutes in this example represents the start-up phase. Figure 5 presents the target final moles of gas, $n_D^{\mathrm{F}}(k)$ in Eq. 26, at each sample time.

The control is initially set to the start-up phase flow rate of 5 mol/min in this example and then is brought to its maximum value when the constraint controller is initiated at 10 min. The control is reduced from its maximum constraint at the end of the recharge when a maximum pressure constraint violation is predicted. The target final moles of gas is determined at each sample period as the amount that results in the predicted tank pressure reaching its maximum constraint. The corrections to this target become larger as the flow rate increases and the tank is filled because the simulated energy losses in the nozzle become larger. We note that measurement noise and initial condition error is not present in this example.

6 Conclusions and Future Work

We have presented a dynamic constraint control approximation to the singular minimum-time optimal control law for recharging high pressure gas storage tanks. This development neglected heat transfer to the storage tank and the surroundings. Although the thermal capacity of the storage tank can reasonably be neglected in the industrial system, heat transfer to the surroundings can become significant with larger changes in both tank temperature and pressure. Future work includes the addition of a thermal model to account for the effect of heat transfer in the thermodynamic model of the system.

Acknowledgments

Support for this work from Air Products and Chemicals Company is gratefully acknowledged.

References

[1] Smith J, Van Ness H, Abbott M (2005) Chemical engineering thermodynamics. 7th ed. McGraw–Hill, New York
[2] Bryson A, Ho Y (1975) Applied optimal control. Taylor & Francis, Levittown
[3] Srinivasan B, Palanki S, Bonvin D (2002) Comput Chem Eng 27(1):1–26
[4] Srinivasan B, Bonvin D, Visser E, Palanki S (2002) Comput Chem Eng 27(1):27–44
[5] Muske K, Badlani M, Dell'Orco P, Brum J (2004) Chem Eng Sci 59(6):1167-1180
[6] Bonvin D, Srinivasan B (2003) ISA Trans 42(1):123–134
[7] Witmer A, Muske K, Weinstein R, Simeone M (2007) Proceedings of the 2007 American Control Conference
[8] Caracotsios M, Stewart W (1985) Comput Chem Eng 9(4):359–365
[9] Christensen R (1996) Analysis of variance, design and regression. Chapman & Hall, London
[10] Zhang W, Schouten J, Hinze H (1992) J Chem Eng Data 37(2):114–119